Macromolecular Delivery into Skin Using a Hollow Microneedle

Nanthida Wonglertnirant,[a,b] Hiroaki Todo,[b] Praneet Opanasopit,[a] Tanasait Ngawhirunpat,[a] and Kenji Sugibayashi*[b]

[a] *Faculty of Pharmacy, Silpakorn University; Nakhon Pathom 73000, Thailand: and* [b] *Faculty of Pharmaceutical Sciences, Josai University; 1–1 Keyakidai, Sakado, Saitama 350–0295, Japan.*

The objective of the present study was to obtain information to develop an effective delivery device regarding a sophisticated hollow microneedle array-patch system. Thus, the potential of hollow microneedles was investigated for enhancing the transdermal delivery of hydrophilic large molecular compounds, and the effect of variable parameters on drug release behavior was determined from skin. Fluorescein isothiocyanate (FITC)-dextrans (4.3 kDa), FD-4, was used as the main model compound, and it was successfully loaded into the lower epidermis as well as the superficial dermis of the skin in hairless rats by a hollow microneedle. The higher the volume of FD-4 solution injected, the faster the FD-4 release rate from skin. In addition, release rate tended to increase when FD-4 was administered dividedly by multiple injections. These release profiles of FD-4 were expressed by Fick's law of diffusion. Furthermore, a combination of the formulation strategy and hollow microneedle-assisted delivery was useful for controlling the drug release rate from skin. Release profiles from drug-loaded skin were also compared by changing the molecular weights of model compounds. The larger molecular size of compounds caused a lower release rate from skin. These results suggest the utilization of hollow microneedle to enhance transdermal delivery of large molecular compounds and provide useful information for designing an effective hollow microneedle system.

Key words   hollow microneedle; drug release; injection; transdermal delivery; large molecular compound

Recently much attention has been paid to a new approach for enhancing transdermal drug delivery employing needles in micron scale, termed microneedles. Such a technique combines the concepts of the user-friendly delivery of transdermal patches and the broad effectiveness of hypodermic injections. Several studies have established the increasing efficacy of microneedle-assisted transdermal delivery for a variety of compounds,[1—4] especially for high molecular weight hydrophilic compounds.[5—7] Microneedles are also expected to be safe, because they are minimally invasive and do not typically cause bleeding or any severe pain at the injection site.[8]

Although microneedles assist in penetrating the stratum corneum (SC) barrier and offer several microchannels facilitating drug transport across the skin, the release of macromolecular drugs at the desired therapeutic rate might not be achieved by only (enhanced) passive diffusion from the patch-based drug reservoir due to the small diffusional area produced by needles.[9] It is necessary to further improve the transdermal delivery of drugs of large molecular weight by contributing push pressure to propel the drug toward the skin, similar to conventional topical injection. Wu *et al.* reported that the combination of solid microneedle pretreatment and subsequent iontophoresis significantly enhanced FD flux compared with microneedle pretreatment alone or iontophoresis alone.[9]

It is difficult, however, to determine the penetration-enhancing effect as well as the parameters affecting the delivery efficiency produced by each enhancing technique and also by each individual microneedle. Yoshida *et al.* carried out a study to investigate the dermatopharmacokinetics (DPK) and systemic drug disposition after topical (intracutaneous (i.c.)) injection of sodium salicylate and concluded that the injection volume was one of the factors which can be utilized to control the drug migration rate from the injection site.[10] Al-Qallaf *et al.* found that different surface areas of the hollow microneedle array-patch system affected the blood concentration of human growth hormone (hGH).[11] Moreover, information on the effect of several factors related to the delivery efficiency of hollow microneedles, for instance, various needle parameters, including injection conditions (*e.g.* length of microneedle/injection depth, needle numbers, distance between each needle, hollow size, pressure of injection, *etc.*), physicochemical properties of drugs (*e.g.* molecular weight, lipophilicity, *etc.*), and formulations must be considered for designing the optimum device.

In this study, we therefore concentrated only on the influence of variables related to the hollow microneedle system on *in vitro* drug release behavior from skin. A single 33-gauge hypodermic needle, where the diameter was almost the same to the arrayed microneedles recently reported,[2,7,9,12,13] was used as a single type hollow microneedle in order to reduce the effect of needle parameters. The effects of injection volume and number of injections on *in vitro* drug release from skin were assessed. Moreover, the effects of formulations and molecular size were investigated.

MATERIALS AND METHODS

Materials   Fluorescein isothiocyanate (FITC)-dextrans (FD-4; average molecular weight, 4.3 kDa) and cholesterol (CH) were purchased from Sigma Aldrich (St. Louis, MO, U.S.A.). Calcein sodium (CAL; molecular weight, 623 Da) was provided by Tokyo Chemical Industry (Tokyo, Japan). Deuterium oxide (D_2O; 99.9%, NMR grade, molecular weight, 20.03 Da) was obtained from Wako Pure Chemical Industries (Osaka, Japan). 1,2-Dimyristoyl-*sn*-glycero-3-phosphocholine (DMPC) was provided by NOF Co., Ltd. (Tokyo, Japan). Disodium ethylenediamine (EDTA·2Na) was purchased from Dojindo Laboratories (Kumamoto,

Japan). Propylene glycol monocaprylic ester (Sefsol-218) and Polyoxyethylene (60) hydrogenated castor oil (HCO-60) were supplied by Nikko Chemicals Co., Ltd. (Tokyo, Japan). All other chemicals were of analytical grade and used without further purification.

Preparation of Hollow Microneedles The hollow microneedles, Nanopass™ (33-gauge hypodermic needle, i.d., 0.20 mm), were kindly provided by Terumo Co. (Tokyo, Japan). A hollow microneedle was manufactured from a microneedle connected to a 27-gauge hypodermic needle (i.d., 0.22 mm; o.d., 0.40 mm; Terumo Co.).

Experimental Animals Male hairless rats (WBM/ILA-Ht, 7—9 weeks-old, body weight: 180—250 g) were supplied either by Life Science Research Center, Josai University (Sakado, Saitama, Japan) or Ishikawa Experimental Animal Laboratories (Fukaya, Saitama, Japan). They were housed in temperature-controlled rooms ($25\pm2\,°C$) with a 12 h light–dark cycle (07:00—19:00 h). The rats were allowed free access to food (M.F. Oriental, Tokyo, Japan) and tap water for a week before experiments. All animal experiments were conducted under the guidelines of Josai University.

The upper part of full-thickness skin was carefully excised from the dorsal region of the rats under anesthesia of intraperitoneally (i.p.) injection of sodium pentobarbital (50 mg/kg), and excess subcutaneous fat was carefully trimmed off. The excised skin, 1.0—1.3 mm in thickness, was immediately used for experiments.

Formulations for Injection To examine the effect of formulations on the drug release behavior from skin after injection by hollow microneedle, three different formulations were considered: solution, o/w emulsion, and liposome suspension. CAL was used as the model drug in this study.

CAL (1 mM) solution was prepared by adding to 1 mM EDTA·2Na in pH 7.4 phosphate-buffered saline (PBS). Emulsion-based formulation was prepared by adding the aqueous phase containing CAL and Sefsol-218 (5%, v/v) to HCO-60 (1%, v/v) in oil phase. Emulsification was carried out using a homogenizer (Polytron® PT3100; Kinematica Inc., NY, U.S.A.) at 13000 rpm for 5 min. The final concentration of CAL in emulsion formulation was 1 mM. Liposome-based formulation was prepared by the reverse phase evaporation method.[14] Briefly, the lipid phase (mixture of DMPC and CH; 7:3, w/w) was dissolved in a chloroform/isopropyl ether mixture (1:1, v/v), and then mixed with the aqueous solution containing CAL (initial concentration 10 mM) in a sonication bath (5510 J-DTH; Branson Ultrasonics Corp., Danbury, CT, U.S.A.) for 5 min to obtain a water-in-oil emulsion. The organic solvent was evaporated under reduced pressure. During this process, the material first forms a viscous gel and subsequently becomes an aqueous suspension. The freeze–thaw cycle was performed and repeated three times. The liposome suspension was then extruded through polycarbonate membranes with pore sizes of 0.4 μm, 0.2 μm, and 0.1 μm, respectively. The extrusion process was run 5 times per membrane pore size. Liposomes were separated from non-encapsulated CAL by ultracentrifugation at 289000×g for 10 min and resuspension of the vesicles in buffer (quadruple). The entrapment efficiency of liposomes was 2.43%. Size distribution was determined by dynamic light scattering (Malvern Instruments, Southborough, MA, U.S.A.) and revealed a mean vesicle diameter of 127.3 nm.

***In Vitro* Skin Release Studies** The extent and rate of drug release from skin were investigated to examine the effect of different four variables (a—d) related to the hollow microneedle-based delivery system on the drug DPK. Unless otherwise mentioned, FD-4 (1 mM) was used as the high molecular compound for testing in this study. *In vitro* release studies were carried out after the following treatments: (1) different volumes of drug solution (5, 10, or 20 μl) were administered into the excised dorsal skin by single injection; (2) different numbers of injections (10 μl single injection, 5 μl two injections, and 2.5 μl four injections) were administered into excised skin. Distance between each injection point was 0.5 cm; (3) different drug formulations (solution, o/w emulsion, or liposome suspension) at 10 μl were injected into excised skin by single injection; (4) different molecular sizes of test compounds (10 μl of either FD-4 (molecular weight (MW) 4300) solution, CAL (MW 623) solution or D_2O (MW 20.03)) were injected into excised skin by single injection.

In the injection process, the skin was stretched onto a cork support board with four tissue-mounting pins to simulate skin tension *in vivo*. The skin containing injected solution was then mounted in a vertical diffusion cell (effective diffusion area: 1.77 cm^2) with the SC side facing the donor compartment (without drug solution), which was covered with Parafilm to establish an occlusive condition. The receiver solution was approximately 6.0 ml of pH 7.4 PBS, which was stirred with a magnetic stirrer bar driven by a constant-speed synchronous motor and maintained at 32 °C using a thermoregulated water bath throughout the experiment. For the release study of CAL, 1 mM EDTA·2Na in pH 7.4 PBS was used instead of pH 7.4 PBS. The receiver solution (0.5 ml) was withdrawn at predetermined time intervals up to 8 h after drug administration, and the same volume of PBS was added to the receiver compartment to keep the volume constant.

After the release study was ended over a period of 8 h, the amount of drug remaining in the skin was measured by isolating the skin from the diffusion cell. The skin was cut into small pieces with scissors and fine forceps, and homogenized (at 12000 rpm for 5 min) with 2 ml PBS to extract the drug under an ice bath. Acetonitrile (2 ml) was then added and mixed with skin homogenized solution using a vortex shaker to precipitate protein. After centrifugation at 15000 rpm for 5 min, the clear supernatant was taken for analysis.

Quantitative Assay The concentrations of FD-4 and CAL samples were analyzed using a spectrofluorophotometer (RF 5300PC; Shimadzu, Kyoto, Japan) at excitation wavelengths of 495 and 490 nm, respectively, and the identical fluorescent emission wavelength of 515 nm. D_2O was determined by the intensity of O-D stretching vibrational band at 2512 cm^{-1} infrared spectroscopic spectra.[9]

Diffusivity of FD-4 in Skin. Analysis of Diffusivity from Drug Release Profiles The hollow microneedle system is defined as a way to directly load drugs into skin and provides a drug depot in skin, as in topical injection. Thus, the DPK after the application of this device may be different from that of conventional topical application.[10] We injected the drug solution into skin by hollow microneedle and observed the drug release behaviors from skin. The obtained release data were analyzed using the empirical mathematical model pro-

posed by Peppas (Eq. 1),[15,16] which is generally used to explain the drug release by coupling Fickian and non-Fickian mechanisms:

$$\frac{M_t}{M_\infty} = kt^n \tag{1}$$

where M_t is the amount of drug released at time t, and M_∞ is the amount of drug released at infinite time. M_t/M_∞ is the fractional drug release, t is the release time, k is a kinetic constant incorporating structural and geometric characteristics of the controlled release device, and n is an exponent which characterizes the mechanism of diffusional release. Based on the exponent, n, drug transport is classified as Fickian diffusion for $n \leq 0.5$, anomalous (non-Fickian) transport for $n > 0.5 — < 1.0$, case II transport or zero order (time-independent release) for $n = 1.0$, and super-case-II transport for $n > 1.0$. This equation is applicable only for data up to 30% of dose release ($M_t/M_\infty < 0.30$). According to Eq. 1, the logarithm of the cumulative amount of drug released each time was plotted against the logarithm of time to calculate n. Release experiments were carried out under perfect sink conditions and release profiles were classified by considering the skin to be a homogeneous single membrane.

Analysis using the Peppas model revealed the primary drug release mechanism of FD-4-loaded skin, which was Fickian diffusion (see Results and Discussion). In this case, the Peppas equation can be expressed the same as the simplified form of the Higuchi diffusion model as follows:

$$Q = kt^{1/2} \tag{2}$$

where Q is the cumulative amount of FD-4 released from the FD-4 loaded skin into the bulk receiver solution per unit surface area (nmol/cm^2), and k is the kinetic constant indicative of the release rate (nmol/cm^2 h$^{1/2}$). Thus, the cumulative amount of drug released is proportional to the square root of time. According to Higuchi, the diffusion coefficient of FD-4 in skin by employing a hollow microneedle as a delivery method, D_{skin} (cm^2/h), can be calculated from Eq. 3.[17]

$$Q = 2C_0 \sqrt{\frac{D_{skin}t}{\pi}} \tag{3}$$

where C_0 is the initial concentration of FD-4 in skin after direct injection (nmol/ml). Equations 2 and 3 are confined to the description of the first 30% of the release curve.

Analysis of Diffusivity from Skin Permeation Profiles To examine the diffusion coefficient of FD-4 in viable epidermis and dermis layers, D_{ved}, stripped skin excised from hairless rats was used as model skin, which was supposed to be a homogenous single membrane (defined as the one-layered diffusion model). The stripped hairless rat skin was set in a diffusion cell, and FD-4 solution was applied to the donor cell on the epidermal side of the skin to determine the skin permeation profiles of FD-4.

The concentration of FD-4, C_{ved}, in the stripped skin at a position, x, and time, t, can be calculated using Fick's second law of diffusion (Eq. 4).

$$\frac{\partial C_{ved}}{\partial t} = D_{ved} \frac{\partial^2 C_{ved}}{\partial x^2} \tag{4}$$

where D_{ved} is the diffusion coefficient of FD-4 in the viable epidermis and dermis layers. Based on the differential equa-

tion, Eq. 4 can be changed to Eq. 5, as described in detail by Hada *et al.*[18] and Sugibayashi *et al.*[19]

$$C_{ved_{i,j+1}} = rD_{ved}C_{ved_{i-1,j}} + (1 - 2rD_{ved})C_{ved_{i,j}} + rD_{ved}C_{ved_{i+1,j}} \tag{5}$$

where $C_{ved_{i,j}}$ is FD-4 concentration at i-th position and j-th time in the stripped skin, r is $\Delta t/\Delta x^2$; Δx is $x_{i+1} - x_i$, and Δt is $t_{j+1} - t_j$. In addition, the skin permeation rate to the receiver compartment, J, can be expressed by Eq. 6. The cumulative amount of FD-4 permeated per unit area, Q, is expressed by Eq. 7.

$$J_j = -D_{ved} \frac{C_{n+1,j} - C_{n,j}}{\Delta x} \tag{6}$$

$$Q_j = Q_{j-1} + J_j \Delta t \tag{7}$$

where n is the number of divisions of skin. Then, J_j was calculated using Microsoft® Excel by setting $n = 10$. Q_j was calculated from J_j using Eq. 7. The diffusion coefficient, D_{ved}, was obtained by fitting the observed data using the least squares method performed by the solver function of Microsoft® Excel. Other conditions of data analysis, not mentioned here, were the same as in the previous study.[18,19]

Full-thickness skin of hairless rats was used instead of stripped skin to calculate the diffusion coefficient of FD-4 in the SC layer, D_{SC}. A two-layered diffusion model was established herein to analyze the FD-4 permeation profiles. FD-4 concentration in the SC layer can be expressed by Fick's second law of diffusion as follows:

$$\frac{\partial C_{SC}}{\partial t} = D_{SC} \frac{\partial^2 C_{SC}}{\partial x^2} \tag{8}$$

FD-4 concentration, C_{ved}, in the viable epidermis and dermis layers at a position, x and time, t can be expressed by Eq. 4. Equation 8 is changed to Eqs. 9 and 10 by differential calculus.[18,19]

$$C_{SC_{i,j+1}} = rD_{SC}C_{SC_{i-1,j}} + (1 - 2rD_{SC})C_{SC_{i,j}} + rD_{SC}C_{SC_{i+1,j}} \tag{9}$$

$$C_{ved_{i,j+1}} = rD_{ved}C_{ved_{i-1,j}} + (1 - 2rD_{ved})C_{ved_{i,j}} + rD_{ved}C_{ved_{i+1,j}} \tag{10}$$

Similar analysis was carried out in the two-layered model using the least squares method to obtain the diffusion coefficient of FD-4 in SC, D_{SC}. In this calculation, diffusivity in the viable epidermis and dermis layers, D_{ved}, was fixed to the already estimated value by the stripped skin permeation experiment.

Histological Imaging To visualize hollow microneedle penetration into the skin and the pathway of fluid injection, a small amount of Evans blue was injected into the skin by a hollow microneedle (Fig. 1B). After removing the microneedle, the skin sample was frozen in isopentane (2-methylbutane) cooled by dry ice with optimal cutting temperature compound (Tissue-Tek; Sakura Finetek, Torrance, CA, U.S.A.) in an embedding mold container. A freezing microtome (Leica CM3050S; Finetec, Japan) was used to make the vertical sections of 10 μm thickness. These sections were examined histologically using a phase-contrast microscope (IX71; Olympus, Japan).

Statistical Analysis *In vitro* drug release measurements were collected from four to six experiments. Values are expressed as the mean±standard error (S.E.). Statistical significance of differences between groups in the amount of FD-4
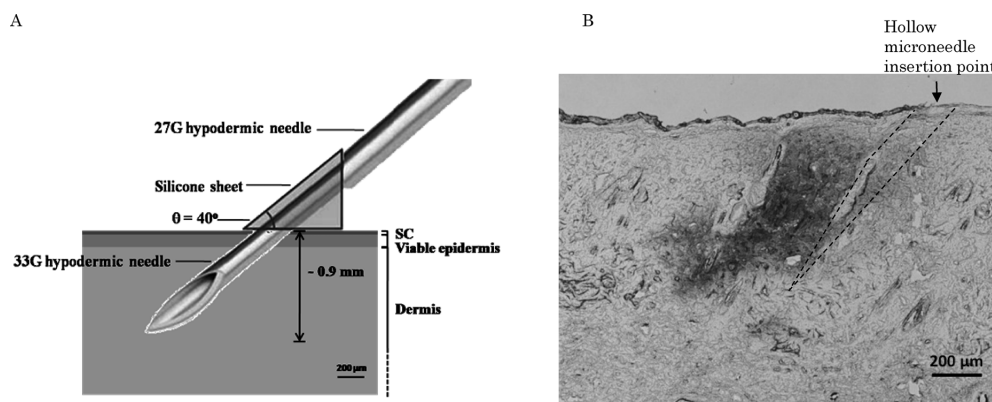
Fig. 1. Schematic Representation of Hollow Microneedle Insertion into Skin with a 33-Gauge Hypodermic Needle (A) and Histological Section of Back Skin of Hairless Rat Pierced with a Hollow Microneedle *in Vitro* (B)

A small amount of Evans blue was injected into skin. The paths of fluid injection are indicated by the presence of blue dye. Dotted lines show where the hollow microneedle was inserted. A hollow microneedle could be inserted forward or backwards in this histological section.

released from skin was examined using one-way analysis of variance (ANOVA) followed by Student's *t*-test. The significance level was set at $p < 0.05$.

RESULTS AND DISCUSSION

Characterization of Hollow Microneedle Injection To investigate piercing of the skin barrier and delivering the drug through the barrier by a hollow microneedle, FD-4 solution was injected into the excised back skin of hairless rats. The needle was fixed with a triangular silicone sheet to maintain an angle of insertion (θ) of 40° and constant insertion depth in the skin barrier, as shown in Fig. 1A. The microneedle tip was inserted easily into the skin using gentle force, and no bending was observed in the needle tip. Up to 20 μl (single injection) of FD-4 solution was successfully injected into skin without any leakage from the skin surface or from the bottom (dermal) side of the skin. The presence of FD-4 solution in skin was visualized by the appearance of a greenish-yellow region spread around the injection site (data not shown). Increasing the injection volume resulted in a broader greenish-yellow region. After injection and removing the needle, the skin was frozen instantly in liquid nitrogen and sectioned vertically to observe FD-4 deposition in the skin.

Next, a histological study was performed by examining skin sections under a light microscope after loading a small amount of Evans blue into the skin using a hollow microneedle. Figure 1B shows a typical cross section of a skin piece. The blue dye in the skin corresponded to the needle insertion across the stratum corneum and upper epidermis as well as into the superficial dermis.

Effects of Injection Volume and Number of Injections on the Release Behavior of FD-4 from Skin To evaluate the effect of the injection volume, 5, 10 and 20 μl FD-4 solution were loaded into the skin using a hollow microneedle. Approximately 80% FD-4 solution was released from the skin over 8 h in all cases (Table 1). Figure 2A shows the time course of the cumulative amounts of FD-4 released per unit area from skin. The obtained drug release profiles were analyzed using the Peppas equation (see 'Diffusivity of FD-4 in Skin') to characterize the release mechanism. Figure 2B shows the double logarithmic plot of the cumulative amount

Table 1. The Percentage of FD-4 Released from Skin over 8 h after Administration by a Hollow Microneedle

Injection volume (μl)	%	Number of injections[a]	%
5	80.2±3.4	1 (10 μl)	81.2±1.6
10	81.2±1.6	2 (each 5 μl)	82.3±1.0
20	84.6±3.4	4 (each 2.5 μl)	85.2±1.2*

a) The total volume of injection was adjusted to 10 μl. *$p < 0.05$ compared with 10 μl single injection. Mean±S.E. with 4 to 6 measurements.

of FD-4 released against time, where slopes of the lines represent the release exponent (n). As a result, a Fickian release can be assumed (n is very close to 0.5). As can be seen in Fig. 2C, linear relationships ($r^2 = 0.974$—0.998) were obtained when the cumulative amounts of FD-4 released from skin were plotted against the square root of time. These results indicated that the release of FD-4 followed the Higuchi diffusion model validated when drug release was less than 30%. The drug release rate (k) can be calculated from the intercept of the Peppas plot. It was shown that increasing the injection volume from 5 to 20 μl increased the release rate almost proportionally (Table 2). Since diffusion in skin was the primary mechanism of drug release from skin, FD-4-loaded skin might be treated as a drug-loaded matrix. In this respect, the Higuchi model (see 'Diffusivity of FD-4 in Skin') was applicable and further used to evaluate the diffusivity of FD-4 in skin (discussed later).

In order to further examine the effect of the number of injections, release studies were performed using different injection conditions, *i.e.* one of 10 μl, two of 5 μl, and four of 2.5 μl. Four 2.5 μl injections showed that a significantly higher amount of FD-4 was released than with one 10 μl and two 5 μl injections ($p < 0.05$) (data not shown). The percentage of FD-4 release from four 2.5 μl injections was also significantly higher than the others, although the total amount of percent FD-4 release at the end of the release period ($t = 8$ h) was not significantly different between four 2.5 μl injections and two 5 μl injections (Table 1). This result might suggest that multiple injections increased total area of FD-4 released from the skin. The effect of the number of injections on drug release was analyzed in a similar manner as above. Thus, the release profiles were also found to follow Higuchi kinetics
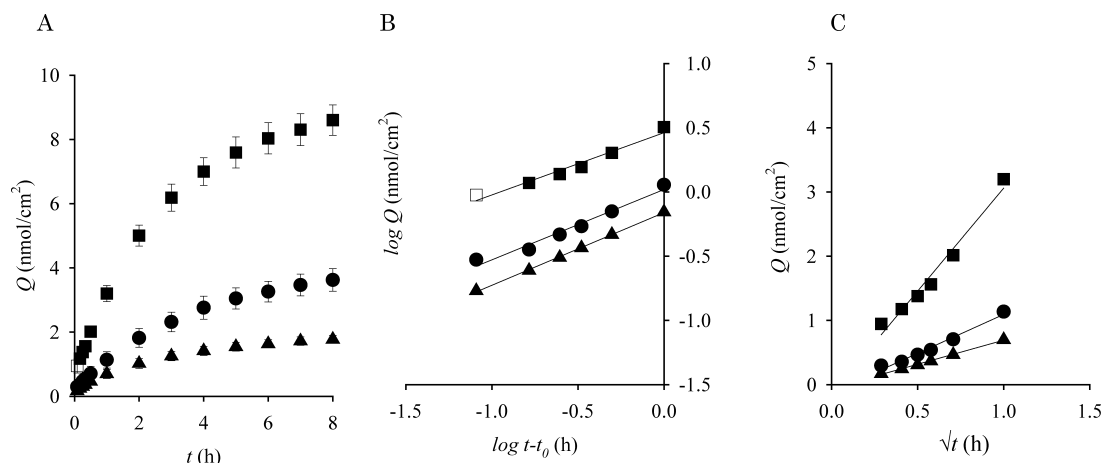
Fig. 2. Effect of Injection Volume on the Release Profile of FD-4 from Skin after Administration of FD-4 Solution of 5, 10 and 20 μl

(A) Accumulated amount of FD-4 released per unit area from skin, (B) and (C) analysis of the effect of injection volume on the FD-4 release profile using Peppas and the simplified Higuchi model, respectively. Symbols: ▲, 5 μl; ●, 10 μl; ■, 20 μl. Solid line represents calculated value. The values in Figs. 2B and C are represented by the following equations, respectively: ▲; $\log Q = 0.56 \times \log t - t_0 - 0.16$ ($r^2 = 0.999$) and $Q = 0.75 \times \sqrt{t} - 0.059$ ($r^2 = 0.998$), ●; $\log Q = 0.53 \times \log t - t_0 + 0.017$ ($r^2 = 0.967$) and $Q = 1.2 \times \sqrt{t} - 0.12$ ($r^2 = 0.979$), ■; $\log Q = 0.48 \times \log t - t_0 + 0.46$ ($r^2 = 0.965$) and $Q = 3.2 \times \sqrt{t} - 0.15$ ($r^2 = 0.974$). Each point represents the mean±S.E. of four to six experiments.

Table 2. Release Kinetics of FD-4 after Administration into Skin by a Hollow Microneedle

	Peppas model $M_t/M_\infty = kt^n$		
	Exponent (n)	Kinetic constant (k)	r^2
Injection volume (μl)			
5	0.556	0.689	0.999
10	0.528	1.040	0.967
20	0.485	2.895	0.965
Number of injections			
1 (10 μl)	0.528	1.040	0.967
2 (each 5 μl)	0.564	0.935	0.965
4 (each 2.5 μl)	0.564	1.345	0.983

($n = 0.528$—0.564). The parameters of n and k derived by the Peppas plot are summarized in Table 2. From the results, dividing the amount of FD-4 loaded into skin by multiple injections was found likely to increase the release rate and total amount of drug released from skin.

Effect of Hollow Microneedle-Assisted Delivery on the Diffusivity of FD-4 within Skin We subsequently examined the diffusion coefficient of FD-4 solution in skin (D_{skin}) from the gradients of Higuchi plots (see 'Diffusivity of FD-4 in Skin'). D_{skin} was calculated to be 6.7×10^{-4} cm^2/h. A comparison was performed with the diffusion coefficient of FD-4 in the stratum corneum layer (D_{SC}) and in viable epidermis and dermis layers (D_{ved}), which were 5.1×10^{-7} and 6.0×10^{-4} cm^2/h, respectively. As a result, D_{skin} was almost the same as D_{ved} and much higher than D_{SC}. Because the SC provides a marked skin barrier, its resistance to drug diffusion in this skin layer is the highest, causing the lowest diffusivity of FD-4. By employing hollow microneedles, the surface of the skin barrier (SC) was bypassed; thus, FD-4 solution was easily delivered into the lower epidermis or dermis, where the permeation resistance of FD-4 must be much lower than that on the SC; therefore, FD-4 can rapidly diffuse through the skin. These results exhibited the utility of hollow microneedles for overcoming the barrier function of SC and enhancing

the delivery of high molecular weight drugs into skin.

Effect of the Different Molecular Sizes of Compounds on the Release Profile from Skin Study of the transport of drug substances within the deeper skin layers lags behind that of transport in SC. Only SC has been recognized as a rate-limiting barrier for skin permeation of drugs, particularly hydrophilic drugs. By employing hollow microneedles, drugs are directly loaded into the lower epidermis or dermis layer and bypass the SC, as explained above. Thus, hydrophilic molecules can be expected to readily diffuse through the lower layers of skin which contain a larger amount of water than the SC. In this study, we then determined the effect of molecular weight on release from skin after administration by hollow microneedles. These studies were conducted with D$_2$O (MW 20.03), CAL (MW 623) and FD-4 (MW 4300). As a result, more than 90.0% D$_2$O was released from treated skin within 2 h (data not shown), and 90.3% CAL was released over 8 h, which was significantly higher than the 81.2% FD-4 released ($p < 0.05$). These results clearly showed that the molecular sizes of drug compounds affect drug release from skin. Alternatively, molecular size has a marked influence on drug diffusivity within the deeper layers of skin, with increasing bulky molecules decreasing in diffusivity.

Effect of Different Formulations on the Release Profile of CAL from Skin We began our discussion by demonstrating the utility of hollow microneedle for transdermal hydrophilic macromolecular delivery and various parameters affecting release behavior from FD-4-loaded skin. Thereafter, the feasibility of different formulations for controlling drug release after loading into skin by hollow microneedles was addressed. For this purpose, three formulations, solution, o/w emulsion, and liposome suspension, were investigated. Although drug delivery by a hollow microneedle system completely evades the barrier function in SC, low diffusion of a large molecular drug through the deeper skin layers may limit drug delivery to the deep epidermis and dermis. To make a logical comparison, therefore, a low molecular weight of the candidate drug was chosen to avoid the problem of skin permeability. Calcein (MW 623) was selected as
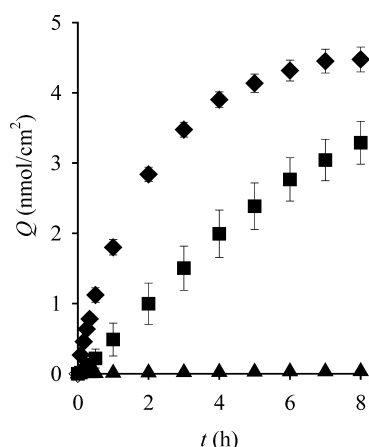
Fig. 3.   Effect of Formulations on the Release Profile of CAL from Skin

Symbols: ◆, solution; ■, emulsion; ▲, liposome. Each point represents the mean±S.E. of four to six experiments.

the penetrant for this comparison. Figure 3 shows different CAL release profiles among three formulations after delivery using a hollow microneedle system. The total amount of CAL released over 8 h was ranked in the order of solution (90.3%)＞emulsion (70.4%)＞liposome (3.6%). As the lipophilic content of the formulation was increased, the drug release considerably declined. CAL was solubilized in the buffer vehicle and in the external phase of oil/water (o/w) emulsion to freely diffuse through the skin, therefore resulting in a greater amount of drug released. In the liposome suspension, CAL release occurred through two steps: i) disrupting vesicle structures in the skin to freely liberate CAL or partitioning of CAL out of lipid vesicles; and ii) diffusion through the skin to bulk receiver solution, together with the rigid vesicle structure of traditional liposomes, which may explain the lower drug release. These results suggest the possibility of controlling drug release from the skin after hollow microneedle administration by employing a formulation strategy.

CONCLUSION

The present study demonstrated the utilization of hollow microneedles for macromolecular drug delivery through skin. We used a single 33-gauge hypodermic needle instead of hollow microneedle array. The needle was inserted into the skin with an angle of 40 degree. The present results may not extrapolate to those by microneedle array. However, the size of 33-gauge hypodermic needle used in this experiment resembles to the hollow microneedle reported by other researchers. Furthermore, both of our device and typical hollow microneedle array could avoid stratum corneum barrier function by creating pores. The advantage of single needle device is capable to investigate several factors such as administration volume, formulation, and depth penetration of needles.

The diffusivity of FD-4 after administration by a hollow microneedle was much larger than that in the SC. Release mechanism of FD-4-loaded skin was found to be Fickian diffusion. Various parameters based on the hollow microneedle system were examined to optimize the delivery device. Overall, the higher the amount of FD-4 delivered, the faster the drug release. Dividing the amount of FD-4 loaded into skin by multiple injections likely increased the total amount of drug released and the release rate from skin. Furthermore, a formulation strategy can be applied with a hollow microneedle system to modify drug release through skin. Further studies are needed to obtain additional details for designing a sophisticated hollow microneedle array-patch system to effectively enhance and precisely control macromolecular delivery across the skin.

REFERENCES

1) Henry S., McAllister D. V., Allen M. G., Prausnitz M. R., *J. Pharm. Sci.*, **87**, 922—925 (1998).
2) McAllister D. V., Wang P. M., Davis S. P., Park J. H., Canatella P. J., Allen M. G., Prausnitz M. R., *Proc. Natl. Acad. Sci. U.S.A.*, **100**, 13755—13760 (2003).
3) Cormier M., Johnson B., Ameri M., Nyam K., Libiran L., Zhang D. D., Daddona P., *J. Controlled Release*, **97**, 503—511 (2004).
4) Al-Qallaf B., Das D. B., Mori D., Cui Z., *Philos. Trans. A Math. Phys. Eng. Sci.*, **365**, 2951—2967 (2007).
5) Martanto W., Davis S. P., Holiday N. R., Wang J., Gill H. S., Prausnitz M. R., *Pharm. Res.*, **21**, 947—952 (2004).
6) Wu X. M., Todo H., Sugibayashi K., *Int. J. Pharm.*, **316**, 102—108 (2006).
7) Verbaan F. J., Bal S. M., van den Berg D. J., Groenink W. H., Verpoorten H., Lüttge R., Bouwstra J. A., *J. Controlled Release*, **117**, 238—245 (2007).
8) Kaushik S., Hord A. H., Denson D. D., McAllister D. V., Smitra S., Allen M. G., Prausnitz M. R., *Anesth. Analg.*, **92**, 502—504 (2001).
9) Wu X. M., Todo H., Sugibayashi K., *J. Controlled Release*, **118**, 189—195 (2007).
10) Yoshida D., Todo H., Hasegawa T., Sugibayashi K., *Int. J. Pharm.*, **337**, 142—147 (2007).
11) Al-Qallaf B., Das D. B., Mori D., Cui Z., *Philos. Trans. A Math. Phys. Eng. Sci.*, **365**, 2951—2967 (2007).
12) Wang P. M., Cornwell M., Hill J., Prausnitz M. R., *J. Invest. Dermatol.*, **126**, 1080—1087 (2006).
13) Harvey A. J., Kaestner S. A., Sutter D. E., Harvey N. G., Mikszta J. A., Pettis R. J., *Pharm. Res.*, 2010, in press.
14) Szoka F. Jr., Papahadjopoulos D., *Proc. Natl. Acad. Sci. U.S.A.*, **75**, 4194—4198 (1978).
15) Peppas N. A., *Pharm. Acta Helv.*, **60**, 110—111 (1985).
16) Costa P., Sousa Lobo J. M., *Eur. J. Pharm. Sci.*, **13**, 123—133 (2001).
17) Higuchi W. I., *J. Pharm. Sci.*, **51**, 802—804 (1962).
18) Hada N., Hasegawa T., Takahashi H., Ishibashi T., Sugibayashi K., *J. Controlled Release*, **108**, 341—350 (2005).
19) Sugibayashi K., Todo H., Oshizaka T., Owada Y., *Pharm. Res.*, **27**, 134—142 (2009).